IEEE Access
Multidisciplinary | Rapid Review | Open Access Journal

IEEE VEHICULAR TECHNOLOGY SOCIETY SECTION

Received 22 October 2023, accepted 30 October 2023, date of publication 7 November 2023, date of current version 13 November 2023.

Digital Object Identifier 10.1109/ACCESS.2023.3330833

RESEARCH ARTICLE

A Digital Twin of Charging Stations for Fleets of Electric Vehicles

ANDRÉ M. B. FRANCISCO[1], JÂNIO MONTEIRO[1,2], AND PEDRO J. S. CARDOSO[1,3]
[1]Instituto Superior de Engenharia, Universidade do Algarve, 8005-139 Faro, Portugal
[2]INESC-ID, 1000-029 Lisboa, Portugal
[3]Laboratory for Robotics and Engineering Systems (LARSyS), ISR-Lisbon, 1049-001 Lisboa, Portugal

Corresponding author: André M. B. Francisco (andrembfrancisco@gmail.com)

This work was supported in part by the Portuguese Foundation for Science and Technology (FCT) through the Individual Research Grant 2021.08754.BD, and in part by the Laboratory for Robotics and Engineering Systems (LARSyS) under Project UIDB/50009/2020.

ABSTRACT The increasing concern over the environmental impact of fossil fuels and associated CO_2 emissions created a growing interest on the use of electric vehicles (EVs) and green energy utilization. In this context, the widespread adoption of EVs should be accompanied by the introduction of generation from renewable energy sources (RES). That insertion, at the distribution level, presents challenges that result from their intermittent nature, requiring demand-response measures that can be addressed by adjusting the charging processes to match the available power. In the framework of EVs renting companies, it is essential to have an efficient charging management that allows achieving high levels of self-consumption and self-sufficiency, lower operational costs and lower payback periods for the investments made. The utilization of digital twins (DTs) can be key to achieve those goals, providing accurate simulations and predictions. Their use in the context of EV charging can offer valuable insights into optimizing charging scheduling and predicting energy demands, taking into consideration distinct scenarios. This paper presents the work done to implement DTs of a set of charging stations (CSs) and EVs, which allow the modeling and improved management of the charging processes of EV fleets, for a set of CSs, integrating RES. In this charging context, experimental results using the DT were applied considering a predicted mobility. The applied scenarios supported an effective and optimized managing performance, reaching low paybacks and high self-sufficiency values. The obtained results show that this method is a viable and cost-effective solution for companies renting EVs.

INDEX TERMS Digital twin, electric vehicles, fleets, smart charging, renewable energy sources.

I. INTRODUCTION

This work puts together RES integration, demand-response strategies, and DT technology to optimize charging station operations. It addresses how these integrated approaches can be used to reshape the future of sustainable transportation.

The exponential growth of the population and the mass industrialization have caused an increase in energy demand [1]. This demand was, and still is, many times fulfilled based on fossil fuels with serious environmental impacts in the CO_2 emissions [2]. A solution to meet this energy demand, while mitigating some of the associated problems, is to increase the amount of energy generated by renewable energy sources (RES). RES has increase by 17% in 2021, standing for more 314 gigawatts (GW) of added capacity. By then, the global power capacity has increased to 3146 GW, with solar photovoltaic (PV) installations increasing nearly 175 GW, reaching a cumulative total of 942 GW. Globally, also for 2021, the estimated share of renewable energy was 28.3% [3].

In this context, the regions at the south of Europe, and in particular of the Algarve's region, in Portugal, due to their location and average daily sunshine hours throughout the year, have a high potential of generating large amounts of energy from PV origins [4]. The high values of solar

The associate editor coordinating the review of this manuscript and approving it for publication was Jie Gao.

radiation, that potentiate greater generation levels in the months that are closer to the summer solstice, are also responsible for a higher amount of touristic influx to these regions during this period of the year. This high correlation between generation and consumption can be used with advantage by touristic infrastructures, including hotel units and electric mobility services, enabling a reduction in energy operational costs.

Yet, renewable energy generation from solar and wind sources are characterized as intermittent resources (IR), due to their variability and difficulty of exact prediction. This characteristic place challenges to the required equilibrium between generation and consumption in electrical grids [5]. At this point, the charging of electrical vehicles (EVs) can be used to compensate the variability of the generation. Thus, if properly managed, the combination between electric mobility and renewable energy generation can promote a stabilization of the electrical grids. In fact, even without considering vehicle-to-grid (V2G) solutions, the flexible characteristics of EVs charging allows the modulation of the charging power according with the energy generated by the RES. I.e., at any given moment, the charging processes can be used by a managing system to cope with the intermittency of the generation. This process can even be complemented by battery units in the EVs charging stations (CSs), that can be used to store the excesses of generation that might exist at certain moments. As expected, due to their high installation costs, the ratio of use of the batteries and of the RES equipment has a direct impact in the period of return of the associated investments, making an efficient management of the fleet of vehicles, in terms of the distribution of charging periods and stations, a critical element in the reduction of the system's costs. Simultaneously, if the installed resources are also optimally managed, the required size of the equipment to install can also be minimized, with an obvious positive impact in the associated return periods. Thus, an optimized fleet management solution has a direct impact in the infrastructural requirements of the CSs, namely in terms of the size of RES equipment to install, allowing a proper dimensioning of the required resources [6], [7].

In the context of EV charging, the demand response measures consist in charging the EVs according with the availability of RES. The so called smart charging of EVs, involves allocating the charging periods of EVs based on the probability of PV energy generation. By doing it, lower amounts of energy are required from the grid and also lower energy surplus is injected in it. This also allows reducing the size of internal batteries of CSs, with a positive impact in the associated costs.

The aforementioned factors support the need for a model and simulation platform where the behavior of the charging infrastructure can be assessed. At this level, a digital twin (DT) is a virtual representation of a physical system or process, that allows real-time monitoring, analysis, and optimization of its performance [8]. By creating a DT of specific electric vehicle charging stations (EVCSs), it is possible to build, assess, and evaluate methods of managing and optimizing the CS operations, before applying them into the production phase. For example, in terms of energy management, by analyzing consumption data, a DT can be used to minimize costs and ensure an efficient energy usage. A DT can also help to supply insights into usage patterns and other key metrics or optimize the EVs charging allocation and PV infrastructure sizing, which has an important role in the global efficiency of the CSs. Overall, a DT helps to further improve efficiency, reduce costs, and reduce payback periods [9], [10].

In this context, this work starts by describing the creation of a DT, based in a physical charging system that exists at the University of Algarve. The charging system integrates battery units, a charge controller, on- and off-grid inverters, PV generation, and allows the control of the charging process of an also existing EV. Based in the modelling of the physical components, a more complex system is then built, with multiple CSs and EVs. The proposed system allows the simulation of the daily EVs dynamics between CSs and their charging management. At a posterior stage, system's simulations allow the computation of the return period of investments made in renewable energy sources, as well as the self-sufficiency (SS) and self-consumption (SC) ratios. The high number of variables involved, in terms of battery sizes and RES to install per CS, together with the definition of the charging periods of each EV and their predictive mobility, make this a non-trivial problem [11].

The developed DTs are supported by a simulation platform implemented in MATLAB. The platform allows testing different configurations of the CSs, including factors such as the generation units, storage capacities, on/off-grid operation, and the evaluation of different charging strategies. I.e., the DT enables the modeling/simulation and optimization of daily EV charging allocation scheduling via the various CSs, considering their PV installation and batteries. In brief, this paper provides a detailed description of the structure and internal parameters of CSs for EV fleets, integrating RES, as well as the description of the equations that manage the relationship between these variables. All this is useful for the implementation of DTs of CSs and EVs.

Using the proposed DT, a case study is then presented that focusses on the use of EVs in urban touristic contexts. The results obtained show that a proper scheduling of EVs charging processes, when combined with an optimized project of generation capacity, allows obtaining shorter periods of return for investments, and higher ratios of SS and SC.

The DT described in this work can be scaled up and implemented on CSs in a variety of locations and configurations. This flexibility allows the creation and integration of a customized charging system in real-world scenarios, which is crucial to maximize an efficient and more sustainable energy management, being one of the paper's main contributions to the state of the art.

To summarize, the contributions of this research work include:

- A detailed model of a CS is made, that integrates RES, batteries and AC/DC charging modes;
- A DT of the whole system is described, comprising several EVs and CSs;
- Given a set of EVs with predicted daily mobility, the DT can be used to optimize their charging periods which results in a better utilization of the available resources, with lower investment needs;

This work distinctively integrates various critical factors, including: 1) Smart charging; 2) Predictive mobility; 3) CS sizing optimization; 4) DT technology; 5) Local storage implementation; 6) RES integration; 7) Comprehensive evaluation metrics incorporating sustainability and payback. Unlike existing literature (see Section II), our approach addresses these elements collectively.

The methodology employed in this study is detailed across various sections of the paper. The data collection methods primarily involve the simulation and evaluation (trough specific metrics to measure system performance) of various test conditions and scenarios. The central tool utilized is MATLAB, which provides a robust platform for constructing and assessing the DT system.

The remaining paper is structured as follows. An in-depth analysis of related work and the technologies that support the current development are summarized in the literature review in Section II. Section III presents the structure and parameters involved in the EVs/CSs energy exchange and the battery model used in this work. Section IV presents the simulation platform, its restrictions, and the evaluation metrics used. Section V describes the implementation of the simulator and its operation and different stages. In Section VI, the test conditions and scenarios are presented, and Section VII presents the results of the case study test. Section VIII discusses and analyzes the results considering some specific tests made. Finally, Section IX concludes this work, discussing future developments.

II. LITERATURE REVIEW

EVs are becoming an increasingly popular alternative to traditional vehicles, particularly as the technology continues to evolve and prices become more competitive. They are an important solution to reduce greenhouse gas emissions and improve air quality in urban areas [12], [13].

However, one of the major challenges associated with EVs is their charging infrastructure, as it requires significant investments in both equipment and software. To have a more efficient, sustainable, and optimized infrastructure, the integration of RES is one of the key elements to consider, bringing several opportunities, but also some challenges. As RES penetration keeps increasing in major urban areas, CSs have the potential to incorporate RES, thereby supporting the current utility grid. In [14] a thorough analysis of EV charging with RES is made. The paper addresses some challenges and proposes several opportunities for future directions of research. The availability of RES is one of the biggest challenges highlighted, together with the integration of smart EV charging mechanisms. For the green transportation goal to be achieved the integration of RES with CSs is essential [15].

Beyond the clear benefit of the environmental impact reduction, the integration of renewable energy sources can increase the electric grid stability and resilience, contributing to a more decentralized infrastructure. The maximization of the usage of generated renewable energy can minimize unnecessary infrastructure investments and reduce costs that result from grid purchases. In this context, several works have already addressed the optimization of the charging of EVs in stations that integrate PV energy sources.

In [16], four different smart charging strategies are analyzed having as case study 78 EV users (with their charging and mobility behaviors) combined with their correspondent rooftop PV generation capacity. When using an optimized charging combined with local storage capacity the average coverage of the EV user demand raised from 56% to 90% or 99%, depending on the smart charging strategy. Still in [16], the importance of a reliable forecast of the EV user demand combined with storage capacity has shown to be essential for reaching better results regarding self-consumption rates.

In [17], a project is presented which simulates an e-bike sharing system that integrates solar supply equipment (with all its system components and user mobility patterns) and energy from the grid. In this specific case this system did not affect the existing conditions in the grid, contributing for the grid voltage stability and reliability. The energy related aspects of the potential of EVCSs powered with solar PV canopies are investigated in [18], with a special focus in its utilization on the parking infrastructure of large-scale retailers. In [19] an algorithm was designed to schedule the EV charging, based on local solar patterns of generation.

A process referred to as smart charging using a rule-based energy management scheme, is proposed in [20]. The solution aims to optimize the utilization of locally generated renewable energy for EV charging, while minimizing the amount and cost of the energy that needs to be bought from the distribution grid, and, by this way, reduce the return periods of the investments made. In [21], the managed self-consumption by EV smart charging schemes, for residential Swedish buildings with PV systems, is assessed. In [22] it is proposed the feasibility of an EV charging system with PV energy. It is noted the importance of technical and economic performance analysis to find the appropriate PV system, with the use of metrics as self-consumption, cost of energy and payback periods.

In [23] the EV charging infrastructure expected to exist in Spain by 2030 is compared with the one that was installed at the end of 2019. In this work, the smart charging process is considered a key technology to accommodate more solar energy input into the electrical grid, reducing the need for, and cost of, grid updates.

Decreasing charging time is one of the key goals to make the EVs charging process more user-friendly. EVs fast direct current (DC) charging is at this level important but require high levels of intermittent consumption. In [24], one megawatt rated CSs with ten EVs capacity is simulated with realistic parameters. Supported in simulations, results show a proper dynamic behavior of the DC bus voltage, the battery voltage, and the battery current, proving that DC fast charging of multiple EVs is feasible.

The integration of renewable energy sources, such as solar and wind, poses multiple challenges to the planning, operation, and control of electrical grids. These challenges arise due to the intermittency of those sources, that are dependent on various factors like weather conditions and time of day [25]. The intermittency can be compensated by using local battery units and keeping a connection to the distribution grid. At this point, these factors are evaluated in [26], where a technical and economic design of a PV and local storage system is assessed. Intermittency can also be compensated using hybrid renewable energy systems (HRES) that, besides combining one or more renewable sources and maintaining a connection to the distribution grid and/or battery units, use conventional energy sources like diesel generators and/or hydrogen systems. At this level, a multicriteria methodology that takes into consideration constraints and includes an experimental stage, to verify the configuration of the HRES for EVs charging stations, is considered in [27]. The system uses a specific software to size and rank (with a multicriteria analysis) possible HRES configurations, after the determination of the available renewable resources and the electricity demand. As another HRES solution, an hydrogen-based domestic microgrid is proposed in [28]. The platform is composed of photovoltaic units, metal hydride hydrogen-based storage with an electrolyzer, and polymeric electrolyte fuel cell, maintaining an interconnection with neighbor grids and electric vehicles. The battery pack model utilized in that work is identical to the one considered in our research.

A good sizing of the PV solar system and storage is essential to achieve good operation levels. A proper PV array sizing ensures that there is enough generation to fulfill the charging demands of the EVs, interconnected with the local batteries to balance energy supply and demand. In this context, several infrastructure sizing optimizations using different methods can be found on literature. For instance, in [29] the authors concluded that the daily measured solar radiation data should be used, instead of monthly average values, to obtain the minimum storage requirements of stand-alone PV systems. The optimal sizing of an autonomous HRES for a V2G parking lot, with PV generation, is performed in [30], based on an heuristic optimization algorithm. Yet, the algorithm does not consider the future demand for power, taking only into account the number of EVs and their states of charge (SoC), as well as the degree SS and the SC ratios.

The optimization of the usage of the CSs by a fleet of EVs should increase the efficiency and optimize other metrics. At this level, in [31] a novel fuzzy integer linear programming and a heuristic fuzzy inference approach (FIA) is suggested for enhancing the efficiency in the CSs utilization. Regarding EV fleet management in parking lots, in [32] a fuzzy logic inference based algorithm (FLIA) is proposed to efficiently manage the available power for EVs. In [33] a fuzzy logic weight-based charging scheme (FLWCS) is proposed to optimize the available power distribution. In the context of a parking lot operator under the operational constraints of the power grid, in [34] a quality of performance (QoP) metric is maximized using a two stage fuzzy logic algorithm. In [35] a decentralized smart charging strategy is proposed with the objective of reducing charging cost for the EV users.

An uncoordinated and uncontrolled charging of EV fleets can affect the stability of the distribution grid [36], [37]. So, the implementation of communication technology is essential to assure better levels of integration between EVs and distribution grid. Regarding the communication mechanisms between the EVs and the charging equipment, including their interoperability, several standards and advanced protocols were created. These standards enable the exchange of relevant parameters between EV and CS, which allows adjusting the load requested from the distribution system, taking into considerations limitations or impositions that can exist at that moment. The communication standard ISO/IEC 15118 is one of the most used and has been in continuous development for this purpose, being specified in [38] and [39]. With the smart charging system included in ISO 15118 is possible to balance the grid's capacity with the energy demand for the increasing number of EVs connecting to the electric grid [40]. In [41] the DC communication standard of ISO15118 and its detailed structure is described and analyzed. In [42] a real-time smart charging, based on precomputed schedules, is assessed as a solution to mitigate the problem of uncoordinated and uncontrolled charging, minimizing electricity cost, peak demand, and load imbalance.

V2G technology allows bidirectional energy exchange between EVs and the electric grid. This exchange offers important services to the grid, such as power regulation, spinning reserve, peak load shaving, load leveling, and reactive power compensation. In this context, V2G technologies and some optimization techniques are reviewed in [43]. In [44] a solution is described that helps to overcome the challenges of the wireless link on V2G communication. A better integration between EVs and electrical grids can be achieved through charge scheduling solutions. For instance, trends in grid integration of future EVs are addressed in [45], discussing ways to reduce that expectable incorporation impact.

In the smart charging scheduling context, mathematical optimization methods and rule based methods were reviewed in [46]. E.g., some methods rely on algorithms that prioritize charging periods of different EVs according with some rule [47], such as the earliest departure first (EDF) method, where

the prediction of the EV departure time is a decisive factor in scheduling.

Application of DTs promises to be a practical solution to address the challenges associated with the operation of an EV fleet system. Although still in the early stages of development, the concept of virtual representation for both the CS and the EV holds a big potential to achieve a more optimized and efficient management of the operation of EV fleets.

The idea of a DT was born at NASA, in the 1960s, as a ''living model'' of the Apollo's mission. Because of an explosion on Apollo 13's oxygen tank and subsequent damage to the engine, to assess the failure, NASA utilized various simulators and integrated digital elements into a physical model of the vehicle [48]. A DT is a computerized replica of a real-life system/product, down to the smallest details, and overall shape and size. It is an intricate virtual model that helps developers, designers, and producers to have a better understanding and perfect the system/product before its creation. As soon as the system/product DT is verified and achieved results according to the goals, the acquired information is applied in real-life to create a physical twin. If all is correctly done, potential unforeseen events will be reduced.

In [8], the concept of DT is separated in two types: digital twin prototype (DTP) and digital twin instance (DTI). A DTP is a type of DT that describes the prototypical physical artifact, having all the informational sets necessary to describe and produce a physical version that duplicates or twins the virtual version. A DTI is a type of DT that detail a specific physical product that an individual DT remains linked to, throughout the life of that physical product.

In this context, for example, a DT can be an EV or a CS, since it is a virtual representation of a physical system (e.g., as presented in [49]). Developing DTs of those system's components, allows to simulate the behavior of the physical system in real-world scenarios and predict how it will perform under different conditions (e.g., see [50]). This information can be used to optimize the design, operation, and maintenance of EVs and CSs. By utilizing a DT, one can simulate various charging scenarios and assess how different charging parameters, such as charging time and speed, affect the station's energy consumption and charging efficiency for different daily charging allocations. In [51] is proposed a smart and cognitive CS architecture with DT parallel intelligence techniques, that allow providing different smart functions as the management of energy, battery health, load, and intelligence and smart user services.

A recent trend is the development of DT ecosystems, where DTs are interconnected to enhance the performance of intricate systems. These systems can range from smart cities and transportation networks to supply chains and agricultural systems (e.g., see [52]). Merging information from several DTs can supply a more thorough comprehension of a complex system and allow for its optimal performance. For example, in [53] a battery dynamic model is validated through experiments on four different types of batteries. The battery models are then integrated into a simulation software and is used in a detailed simulation of an EV with a hybrid fuel cell-battery power source. The paper also presents an interesting review of recent developments focused on the use of DTs in electromobility and autonomous vehicles.

In [54] a review is presented that discusses the latest developments in DT technology in smart EVs. The review emphasizes the advantages of DT technology but also acknowledges the challenges it might face in expanding its use. In [55], a thorough overview of how DT technology can revolutionize EVs applications is presented. It addresses key challenges in EV services like tracking, monitoring, battery management, connectivity, security, and privacy.

The current state of the literature regarding DT in EV and EVCS context reveals to be short. The concept of DT has been increasing recognition over various industries. In the specific domain of application to EVs and its infrastructure still remains relatively underexplored. Further research is needed to enhance the full extent of DT capabilities in EV charging optimization and solving issues related to uncoordinated charging.

In Table 1, a comparative analysis of the key works referenced in this section is made, concerning the following topics: (1) Smart charging; (2) Predictive mobility; (3) CS sizing optimization; (4) DT implementation; (5) Local storage; (6) RES integration; (7) Utilization of sustainability parameters and payback as evaluation/performance metrics. The constructed comparative review table aims to allow an easy identification of the covered areas in the works included in this state-of-the-art section. By juxtaposing specific primary topics across the selected references, we gain valuable insights into areas where advancements or further research are needed.

The following section will present the base architecture and specifications of the DTs for the CS and EV developed in this study.

III. MODELING OF A CHARGING STATION AND ELECTRIC VEHICLES

This chapter describes the architectural structure of the proposed charging system, which comprises a real CS, an EV, and corresponding DT. The DT is connected with the physical devices (CS and EV) through a communication system, which allows real measuring of several parameters of the associated equipment and controlling the charging process of the EV. The DT models the whole system and allows predicting the SoC of the batteries in the CS and EV, according with the real and/or simulated variables and actions. So, given an initial state, the DT allows performing several what-if tests, which can be used to optimize the charge control.

In the following sections we specify the electrical parameters involved in the architectural model of the CS. Then, the

TABLE 1. Comparative review of key references regarding the primary topics of this work.

Ref.	Smart charging	Predictive Mobility	CS sizing optimization	DT	Local storage	RES integration	Evaluation metrics	
							Sustainability	Payback
[16]	✓	✓			✓	✓	✓	
[17]	✓	✓			✓	✓		
[19]	✓				✓	✓		
[20]	✓		✓			✓		✓
[21]	✓					✓	✓	
[22]	✓		✓		✓	✓	✓	✓
[24]	✓							
[27]	✓		✓		✓	✓	✓	✓
[28]	✓				✓	✓		
[30]	✓		✓		✓	✓		✓
[42]	✓	✓						
[47]	✓				✓	✓	✓	✓
[51]	✓			✓	✓	✓		
This work	✓	✓	✓	✓	✓	✓	✓	✓

constraints concerning the power flows in the different buses and elements are defined. Finally, in Section C we describe the battery model that was used for both the EV and CS DT.

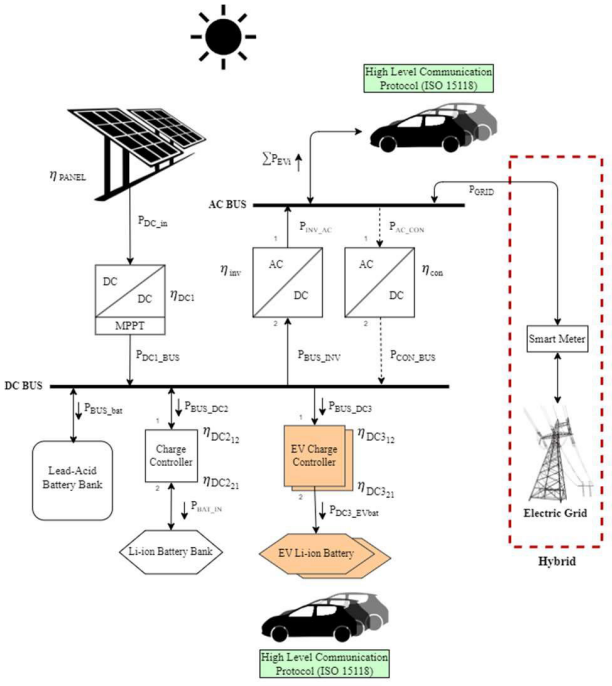

FIGURE 1. Architecture of a CS, which integrates renewable energy sources and comprises two buses (AC and DC), allowing either on or off-grid operation.

A. ARCHITECTURE

Fig. 1 presents the architecture of the CS considered in this work, with the real CS devices and the PV array shown in Fig. 2. The proposed scheme aims to serve as a base for a station that allows EV charging (in AC and DC) using energy from solar PV generation. The CS's architecture, shown in Fig. 1, consists of two buses, one DC and another AC. A PV array feeds the CS, through a maximum power point tracking (MPPT) converter (DC_1) that is used to optimize the power going into the DC bus. In the DC bus, a lead-acid battery is used to balance the voltage. Depending on the number of charging points, at least two more converters are implemented for different purposes, namely: to charge the CS battery bank (DC_2) and to fast charge the EVs in the system (one converter per EV, aggregated in the model as DC_3). In the AC bus there is an inverter (DC to AC), so the power can flow from the DC to the AC bus, and an AC to DC converter, for the opposite flow. Distinct power flows can exist between all these elements and will be mentioned next.

The system allows either an off-grid or an on-grid mode, i.e., it can be connected to the distribution grid, so it could feed it or be fed from it. Table 2 summarizes the variables that characterize the system, as shown in the diagram depicted in Fig.1, which will be used ahead in the description of the system.

B. POWER FLOWS

In the following, we describe the relations between the flows for both the AC and DC buses.

FIGURE 2. CS at the University of Algarve, comprising: (A) PV array and (B) battery units, on and off-grid inverters, and charge controller. (C1) EV and (C2) EV battery storage with SoC monitorization.

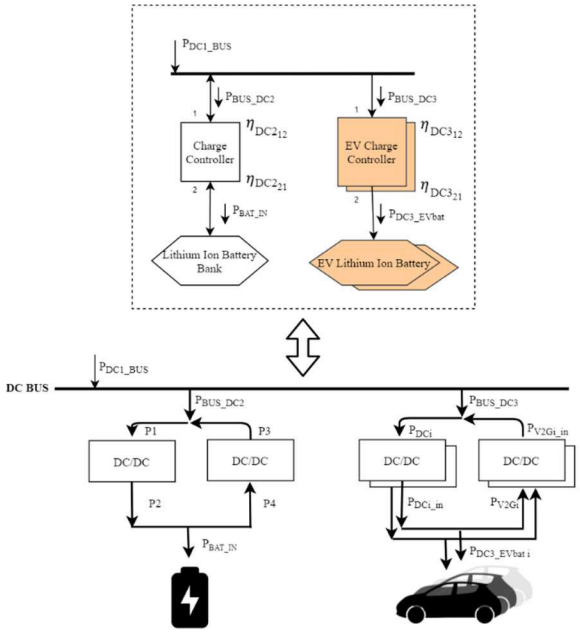

FIGURE 3. Power flows between the DC bus and Li-ion batteries: on the top are the architecture's modules and on the bottom the representation of the admissible power flows.

TABLE 2. Variables used.

Name	Meaning
P_{RAD}	Irradiated power received by the PV array
P_{DC3_EVBAT}	Power input of the EV batteries
P_D	Power output of the PV installation
$P_{BUS_{INV}}$	Power input of the inverter
P_{DCi_BUS}	Power output of the DC converter i to the DC BUS
P_{BUS_DCi}	Power input of the DC converter i from the DC BUS
P_{INV_AC}	Power output of the inverter to the AC BUS
P_{BAT_IN}	Power input of the battery bank
P_{AC_CON}	Power input of the AC converter from the AC BUS
P_{CON_BUS}	Power output of the AC/DC converter to the DC BUS
P_{GRID}	Power input/output of the grid
P_{EV}	Power input of the EV
P_{BUS_bat}	Power input of the lead acid battery bank from the DC BUS
η_{PANEL}	Efficiency of the PV panel
η_{DCi}	Efficiency of the DC converter *i*
η_{inv}	Efficiency of the inverter
η_{con}	Efficiency of the AC/DC Converter

1) DC BUS

In the DC bus, the power that enters the system ($P_{DC_{in}}$) from the PV generation results from the conversion of the radiated power from the sun into electrical power. After passing through the MPPT converter, the power injected into the DC bus is obtained from:

$$P_{DC1\_BUS} = P_{DC\_in}.\eta_{DC_1}, \quad (1)$$

where η_{DC_1} translates the efficiency of the DC_1 converter. The relations between the power inputs and outputs on the DC bus, as represented in Fig. 1, are given by:

$$P_{DC_{1\_BUS}} + P_{CON\_BUS} = P_{BUS\_DC2} + P_{BUS\_bat} + P_{BUS\_DC3} + P_{BUS\_INV}, \quad (2)$$

where P_{CON_BUS} translates the power output of the AC/DC converter, P_{BUS_DC2} translates the power input of the DC_2 converter, P_{BUS_bat} translates the power input of the lead acid battery bank, P_{BUS_DC3} translates the power input of the DC_3 converter, and P_{BUS_INV} translates the power input of the inverter.

The lead-acid battery pack is intended to keep the bus voltage stable. This battery unit has an associated maximum capacity (expressed in kWh or Ah) as well as a maximum charge/discharge power. The voltage at the battery unit input, V_{bat}, which is equal to the DC bus voltage, is given by [56]:

$$V_{bat} = V_{btint} - I_{bt}.R_i, \quad (3)$$

where I_{bt} translates the output current from the battery, R_i the internal resistance of the battery, and V_{btint} the internal voltage of the battery. In Section C, the lead-acid battery model will be presented in more detail, allowing the computation of the internal voltage of the battery (V_{btint}) values.

The $P_{BUS_{bat}}$ is the power from the battery and is defined as positive in the charging process and negative in the discharging case, so it is related to output current from the battery (I_{bt}) through expression:

$$P_{BUS_{bat}} = -I_{bt}.V_{bat} \quad (4)$$

The DT extends the physical structure of the CS by also allowing the modelling of Li-ion batteries. Regarding the charging and discharging systems of the lithium-Ion batteries, Fig. 3 presents, with more detail, the associated power flows.

As with the station's internal storage, at any given moment, Li-ion batteries can either be charging, discharging, or in an idle state. Thus, power flows P_1 and P_3 (power injected in the battery bank before converter and power from the battery bank after converter, respectively) are mutually exclusive. The same occurs between P_2 and P_4 (power injected in the battery bank after the converter and power from the battery bank before the converter, respectively), P_{DCi} and $P_{V2Gi_{in}}$, etc. In an idle state these power flows are equal to zero, as for instance happens when the battery unit is at its maximum capacity.

In terms of the nodes of the station's Li-ion battery, the equations that relate these variables are:

$$\begin{cases} P_1 = P_{BUS\_DC2} + P_3 \\ P_2 = P_1.\eta_{DC2_{12}} \\ P_2 = P_4 + P_{BAT\_IN} \\ P_3 = P_4.\eta_{DC2_{21}} \end{cases} \quad (5)$$

where P_{BUS_DC2} is the power in the converter of the internal storage in Li-ion batteries, P_{BAT_IN} stands for the power in the actual battery (input if positive and output if negative, for both variables) and $\eta_{DC2_{12}}$ and $\eta_{DC2_{21}}$ translate the efficiency of both directions of the flow in the internal battery.

Regarding the EV charging modules, the powers are given by:

$$P_{BUS\_DC3} = \sum_i P_{DCi} - \sum_i P_{V2Gi_{in}}, \quad (6)$$

where P_{BUS_DC3} represents the DC power (input or output) of the EV, P_{DCi} represents the input power of the DC load converter, and $P_{V2Gi_{in}}$ represents the DC power from each EV i that is connected with the system.

Additionally, for each EV i the following equations stand:

$$\begin{cases} P_{V2Gi_{in}} = P_{V2Gi}.\eta_{DC3_{21}} \\ P_{DCi_{in}} = P_{DCi}.\eta_{DC3_{12}} \\ P_{DCi_{in}} = P_{DC3_{EVbat_i}} + P_{V2Gi} \end{cases} \quad (7)$$

where $P_{DC3_{EVbat_i}}$ is the input power that charges the EV and $\eta_{DC3_{21}}$ and $\eta_{DC3_{12}}$ are the efficiency from both directions of flow of the EV converter (in this work, V2G is not considered).

Given the restrictions of power flows, it is up to the management algorithm to decide which devices are active at any given instant, and the values of the input and output of the bus (output value of the MPPT converter and the input of the EV charge controller).

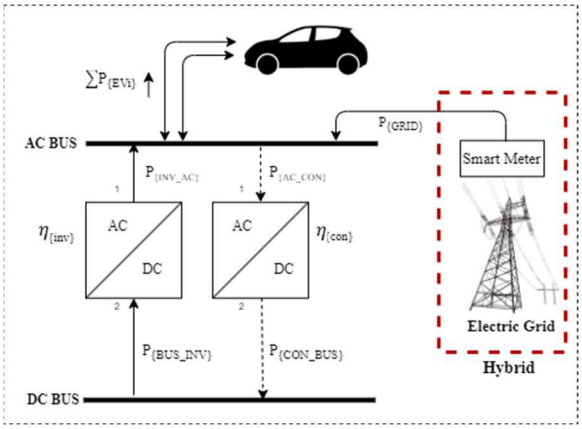

FIGURE 4. Power flows on the AC bus and its interconnection with the DC bus.

2) AC BUS

On the AC bus, represented in Fig. 4, there are several power flows that are related. These relations will be presented in the following.

The DC/AC inverter allows the flow of power between the DC and the AC buses, according with:

$$P_{INV\_AC} = P_{BUS\_INV}.\eta_{inv}, \quad (8)$$

where P_{INV_AC} is the power output of the inverter and can be used by the EV supply equipment in AC and/or be injected into the distribution grid, allowing the selling for financial purposes.

The AC/DC converter allows the flow of power between the AC and the DC buses, according with:

$$P_{CON\_BUS} = P_{AC\_CON} . \eta_{con}, \tag{9}$$

where P_{CON_BUS} can be used by the EV supply equipment in DC and/or injected into the local storage battery.

Considering the scheme in Fig.4, the AC bus flows equality and can be represented as:

$$P_{GRID} + P_{INV\_AC} = P_{AC\_CON} + \sum_{i=1}^{\#EVs} P_{EVi} \tag{10}$$

where P_{GRID} translates the AC power coming from the distribution grid, P_{INV_AC} represents the power received by the inverter, $P_{AC_{CON}}$ is the power injected in the AC/DC converter, $\#EVs$ is the number of EVs, and P_{EVi} represents the power used by each charging point i. In an off-grid scenario, P_{GRID} will always be equal to zero since there will be no connection to the distribution grid.

3) BATTERY MODEL

The model used for estimation of the SoC of the EVs CS battery is based in a lead-acid battery model, which is characterized by an internal resistor R_i, in series with an internal voltage source, following Equation (3).

The following mathematical deductions (based in [57], [58], [59]) allow us to derive a general expression for the battery's internal voltage, V_{btint}. Through the carried-out analysis, the following assumptions were made: (1) the anode and cathode of the cell have porous active materials, (2) electrolyte resistance is constant during discharge, (3) the cell is discharged by a constant current, and (4) polarization is a linear function of the current density of the active material.

In this context, the battery modelling requires to consider several parameters. The maximum capacity, C_{bt}, and the internal resistance of the battery, R_i, can be found in the batterie's specifications table. The remaining parameters are derived from the characteristics of the typical discharge curve, plotted in Fig.5, in steady state, which the battery manufacturers provide in the equipment's datasheets. These parameters are approximated and depend on the accuracy of the points obtained on the discharge curve. The battery's parameters used in this model are summarized in Table 3. The battery's internal voltage during the charging process, stated in [58], is represented as:

$$V_{btint} = V_{bt,0} - K_{bt} . \frac{C_{bt}}{C_{out} + 0.1.C_{bt}} . I_{bt} - K_{bt} . \frac{C_{bt}}{C_{bt} - C_{out}} . C_{out} + A_{bt} . e^{-B_{bt} . C_{out}}, \tag{11}$$

where I_{bt} is the output current from the battery and must be negative, $V_{bt,0}$ translates the voltage at the end of the exponential zone, C_{bt} translates the maximum capacity of the battery, C_{out} translates the extracted capacity, K_{bt} translates the polarization constant, A_{bt} translates the exponential zone's amplitude, and B_{bt} translates the exponential zone's inverse time constant.

TABLE 3. Model parameters of a battery.

Parameters	Meaning
C_{bt}	Maximum capacity (Ah)
C_{out}	Extracted capacity (Ah)
$V_{bt,0}$	Constant voltage (V)
K_{bt}	Polarization constant (V)
A_{bt}	Exponential zone amplitude (V)
B_{bt}	Exponential zone inverse time constant $[Ah]^{-1}$
R_i	Battery internal resistance (Ω)

In the discharge process [58], the internal voltage of the battery is represented by:

$$V_{btint} = V_{bt,0} - K_{bt} . \frac{C_{bt}}{C_{bt} - C_{out}} . I_{bt} - K_{bt} . \frac{C_{bt}}{C_{bt} - C_{out}} . C_{out} + A_{bt} . e^{-B_{bt} . C_{out}}, \tag{12}$$

where I_{bt} must be positive.

In Eqs. (11) and (12), $A_{bt} . e^{-B_{bt} . C_{out}}$ translates the voltage decay in the exponential zone and A_{bt} is the exponential zone amplitude (in Volts) given by:

$$A_{bt} = V_{Full} - V_{bt,0}, \tag{13}$$

where V_{Full} translates the full charge voltage. The inverse of the exponential zone time constant (B_{bt}) (described how to obtain in [57]) where V_{Full} translates the full charge voltage. The inverse of the exponential zone time constant (B_{bt}) [57] is obtained by:

$$B_{bt} = \frac{3}{C_{Exp}} \tag{14}$$

where C_{Exp} represents the capacity at the end of the exponential zone (in Ah). The capacity extracted from the battery, C_{out}, is obtained from [28], where C_{Exp} represents the capacity at the end of the exponential zone (in Ah). The capacity extracted from the battery C_{out} [28], is obtained from:

$$C_{out} = \int_0^t I_{bt} dt. \tag{15}$$

Finally, in the modeled battery system, done in this work, Eq. (15), is approximated by the numerical integration, using the minute as a time basis, through:

$$C_{out} = \int_0^t I_{bt} dt \approx \frac{1}{60} . \sum_{t=0}^{t_f} I_{bt}(t), \tag{16}$$

where t_f corresponds to the final minute of the discharge period.

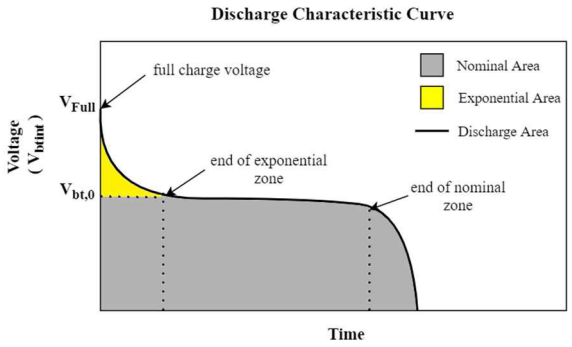

FIGURE 5. Typical discharge curve adapted from [58].

IV. SYSTEM CONSTRAINTS AND EVALUATION METRICS

As introduced in Section I, the aim of this work is to define, characterize and implement a DT and associated simulator that allows modeling and semi-optimize the charging infrastructure. The system is applied in the context of a fleet of EVs, to be rented in touristic areas. The simulated infrastructure comprises several CSs and a set of EVs. The CSs and EVs are based in DTs of CSs and EVs, respectively, that exist at the University of Algarve. The simulation environment can thus be used in two ways, namely: (1) to simulate a system that comprises nonexistent CSs and EVs or (2) to create a large DT of already existing CSs and EVs. The aim of both scenarios is to create a decision support system for the evaluation of investments made in RES and/or management strategies.

So, in this section, we focus on the digital simulation of a system that comprises nonexistent CSs and EVs. The aim of the digital system is to allow the optimization of the: (1) size of the renewable energy equipment to install and (2) the scheduling of the charging periods of the EVs, to allow the maximization of the utilization of the energy that is locally produced, for on and/or off-grid stations.

In this context, the objective of this section is to present the working restrictions and the evaluation metrics of the simulation platform, built in MATLAB. The location of each CS and the characteristics of the equipment installed in each one, can be made to vary.

A. RESTRICTIONS IMPOSED ON THE OPERATION

There are some restrictions that must be followed in each station to ensure that the energy from the local PV generation is used mainly for the EVs charging, and only the surplus energy is sent into the internal batteries of the CSs. It should also guarantee that the SoC limits of batteries are respected. The rules are summarized in Table 4, distinguishing between on-grid and off-grid CSs.

B. EVALUATION METRICS

The evaluation of the solutions that result from the scheduling of EVs and of the investments made in renewable systems, require the use of some quantification methods. These methods can be divided into two groups: financial and of energy flow [60].

In the financial scope, an estimate is made of the annually saved cost by introducing RES and the profits that may result from selling part of the generation. Both, savings and profits, are used to compute the payback of the system, whose value (e.g., in years or months) translate the period required to recover the initial investment and start making a profit. The payback period is computed by dividing all the costs by the yearly/monthly/daily savings plus profits.

In terms of energy flow methods, the self-sufficiency (SS) and the self-consumption (SC) ratios are normally used to allow the quantification of whether the production, storage, or consumption ratios are adequate.

TABLE 4. Control options of the cs depending on the generation availability and/or on/off-grid operation.

	On-grid operation	Off-grid operation
PV not producing energy	**If EVs are scheduled to charge**	
	The battery of the CS is used to charge the scheduled EVs at their maximum power, until batteries SoC reaches 20% (i.e., SoC ≤ 20%); In case there is not enough power to supply the demand, the rest is obtained from the distribution grid.	The Internal battery of the CS charges the scheduled EVs, until battery SoC ≤ 20%.
	Without EVs scheduled to charge	
	The internal battery of CS maintains its SoC.	

	On-grid operation	Off-grid operation
PV producing energy	**If EVs are scheduled to charge**	
	Scheduled EVs are charged using energy from the local generation; In case there is not enough power to supply the demand, the remaining power is obtained from the distribution grid; If there is a surplus of power coming from generation: (1) it is used to charge the internal battery of the CS up to its defined maximum SoC (90-99%); (2) the remaining energy is sold;	Scheduled EVs are charged using energy from the local generation and from the batteries of the CS; If there is a surplus of power coming from generation, it is used to charge the internal battery of the CS up to its defined maximum SoC (90-99%); When the SoC of the internal battery reaches its maximum level, $P_{DC1_{BUS}}$ must be forced to 0.
	Without EVs scheduled to charge	
	Generation is used to: (1) charge the internal battery of the CS up to its defined maximum SoC (90-99%); (2) the remaining energy is sold.	Generation charges the internal battery of the CS up to its defined maximum SoC (90-99%). When the SoC of the internal battery reaches its maximum level, $P_{DC1_{BUS}}$ must be forced to 0.

These metrics are described in the following section.

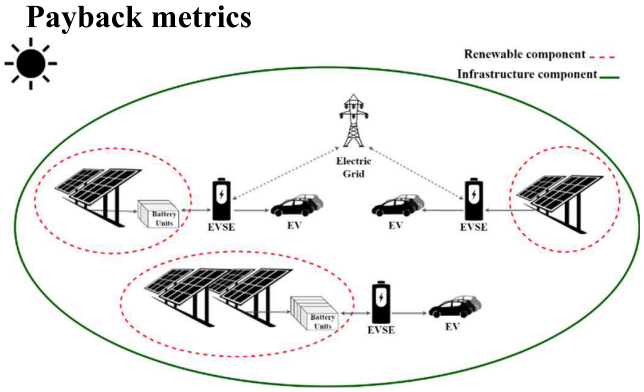

FIGURE 6. Equipment considered for the computation of the Renewable payback and for the Infra-structure payback.

1) PAYBACK METRICS

For the computation of the payback, several components need to be considered: (1) the total cost of the investment, which is obtained by summing the costs of all components of the system, including installation; (2) the savings, resulting from the generated/consumed energy that is not purchased from the grid [61]; (3) the profit that results from the car renting services; and (4) the selling the surplus of the generated energy.

Fig.6 characterizes the types of investments involved in a charging system and fleet of EVs, that integrate RES. It is possible to divide the system payback into two components: renewable payback and infrastructure payback.

The renewable payback is only associated with the investments made in renewable energy sources, including PV units and storage systems, in some or all the CSs. It can be obtained by the following equation:

$$\begin{aligned} &\textit{Renewable payback} \\ &\quad = \frac{\textit{Investment in the renewable enersy system}}{\textit{Monthly renewable generation profits}} \\ &\quad [\textit{months}] \end{aligned} \tag{17}$$

The monthly renewable generation profits result from:

$$\begin{aligned} &\textit{Monthly renewable generation profits} \\ &\quad = \textit{Renewable savings} + \textit{Grid selling}, \end{aligned} \tag{18}$$

where the *Renewable savings* translates the monthly savings obtained by not purchasing energy from the grid due to the renewable energy generation (either directly or from a temporary energy stored in a CS battery) and *Grid selling* translates the monthly revenue obtained from selling the surplus of the generated energy to the distribution grid, the *Grid selling* will only happen in on-grid CSs.

The infrastructure's payback is obtained through:

$$\textit{Infrastructure payback} = \frac{\textit{Total investment}}{\textit{Monthly profits}}\,[\textit{month}] \tag{19}$$

where the *total investment*:

$$\begin{aligned} \textit{Total investment} &= \textit{Renewable energy system cost} \\ &\quad + \textit{Equipment cost} \end{aligned}$$

where the *Equipment cost* is all the equipment needed apart from the PV and storage units.

and

$$\begin{aligned} \textit{Monthly profits} &= \textit{Renewable savings} \\ &\quad + \textit{Grid selling} + \textit{Rental services} \\ &\quad - (\textit{Operation cost} + \textit{Maintenance cost}) \end{aligned}$$

is obtained by summing up the costs of all investments, including RES, but also all the equipment of the CSs and EVs. The monthly profit is obtained from the monthly generation income, rental services, minus the maintenance costs and operation costs, the latter of which are the costs of purchasing energy from the distribution grid.

2) ENERGY FLOW METRICS

In terms of energy flow metrics, two of the most common parameters used are the SC and SS ratios. To compute them, the following components need to be taken into account [60]: (1) the amount of energy generated in the PV system; (2) the amount of renewable energy consumed directly, i.e., used directly to charge the batteries of the EVs; (3) the amount of self-consumed energy, considering both the energy generated by the PV unit and also the one obtained from battery storage; and (4) the amount of energy consumed from the grid.

The direct SC ratio translates the percentage of the amount energy that is directly consumed, without going through the battery unit. Given an interval of time $[t_i,\ t_f]$, the direct self-consumption ratio, q_{DSC}, is computed using [60]:

$$q_{DSC} = \frac{\int_{ti}^{tf} P_{DSC}(t)dt}{\int_{ti}^{tf} P_{PV}(t)dt}, \tag{20}$$

where P_{DSC} represents the generated power that is directly self-consumed and P_{PV} the PV power generated in the same period.

By adding a bank of batteries to the system, the self-consumed energy increases, as the excess energy can be stored in the batteries for later use. Storage typically allows an increase on the amount of energy used locally.

In this context, the non-direct self-consumption ratio or simply, the SC ratio, defines the amount of PV energy that can be consumed locally, using both the PV system and storage, as a percentage of total solar generation [60]. Given a period of time $[t_i,\ t_f]$, the SC ratio, q_{SC}, is computed using:

$$q_{SC} = \frac{\int_{ti}^{tf} P_{SC}(t)dt}{\int_{ti}^{tf} P_{PV}(t)dt}, \tag{21}$$

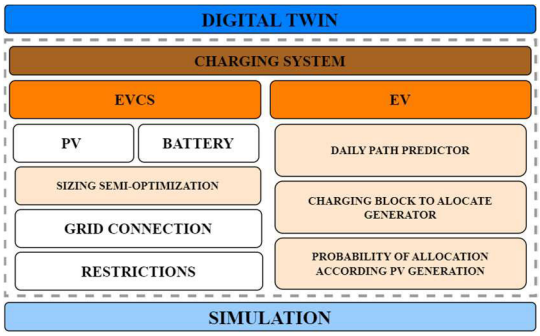

FIGURE 7. Block architecture of the digital twin with custom functions for the case study formulation.

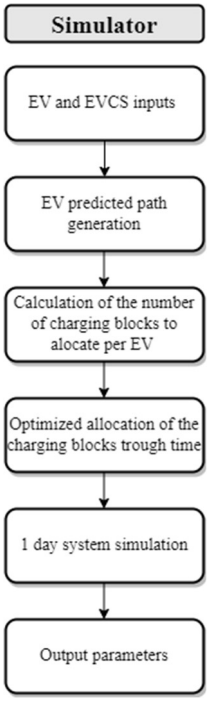

FIGURE 8. Stages flowchart of the simulator.

where P_{SC} represents the generated power that is self-consumed directly and/or from local battery units, in the same period.

The degree of SS translates the ratio between the generated energy that is self-consumed and the total consumed energy in the installation. Given an interval of time $[t_i, t_f]$, the degree of SS, q_S, is computed using:

$$q_S = \frac{\int_{ti}^{tf} P_{SC}(t)dt}{\int_{ti}^{tf} P_{Load}(t)dt}, \tag{22}$$

where P_{SC} represents the self-consumed PV power (directly and/or from local battery units) and P_{Load} translates the consumed power.

Certainly, a perfect system has SC and SS both set at an optimal 100%.

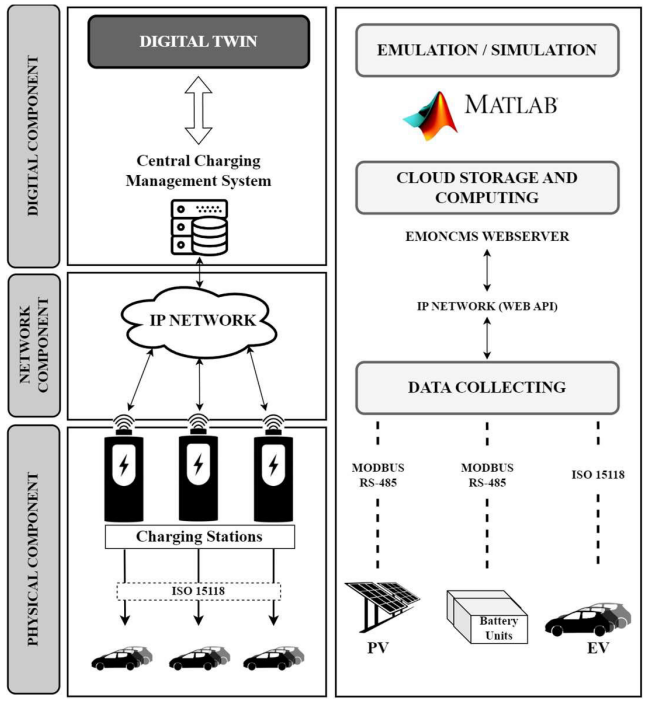

FIGURE 9. Architecture of the digital twin with the correspondent different layers of the system and the communication protocols used.

V. DIGITAL TWIN SIMULATOR

In this section the operation and the different stages of the DT simulator are described. As mentioned in the previous section, the simulator was developed in MATLAB. With its flexibility and robusteness, the MATLAB based EV charging system simulator can provide a valid representation of various scenarios, considering numerous factors and constraints (Fig.7 presents the DT blocks architecture). Fig. 8 presents the different stages of the simulator, which are presented in subsection C. The flowchart shown in Fig. 8, portrays a simplified structure, intentionally designed to provide a clear and concise overview of the algorithm's primary steps. Each stage from the flowchart corresponds to a specific MATLAB function. Fig. 9 shows the DT architecture with the corresponding different layers of the system. These three layers work together to create a dynamic DT model. The physical layer is the foundation for creatting a precise virtual representation. It can have various types of data sources, namelly: (1) Real-world data; and (2) Predictions and forecasts. When dealing with complex scenarios, predictive models and algorithms may be applied.

The network layer facilitates communication between both the physical and the digital layer. At the top of the architecture, the digital layer processes the data received from the network layer to create the virtual replica. The different communication technologies and protocols used are also presented in this figure.

This architecture enables performing simulations, prediction's analysis, real-time monitoring, and optimization of the physical system.

A. INPUTS

The implemented simulator has several input parameters, summarized in Fig.10, that allow its application in different scenarios, with distinct restrictions. These parameters are divided in three main categories, namely: (1) base parameters, (2) economic parameters, and (3) parameters related with grid interconnection. At the base level, the model allows the selection of the number of EVs, the number of CSs, together with the parameters that characterize each CS, including the sizes of the battery and of the PV units. The tariff rates of the energy bought from the distribution grid, the per kWp cost of the PV installation, and the per kWh cost of the battery installations in each CS define the economic parameters. For on-grid CSs, the contracted power and maximum power that can be injected upwards (i.e., from the CS to the distribution grid) can also be specified.

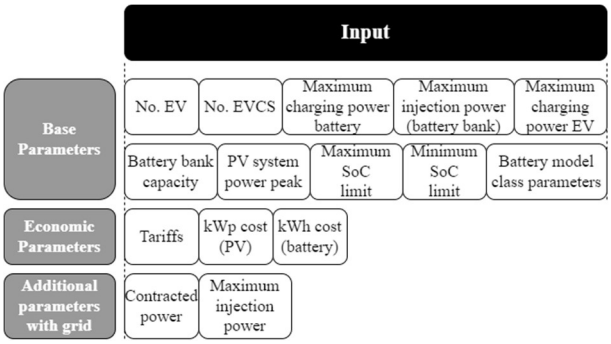

FIGURE 10. Input parameters of the simulator.

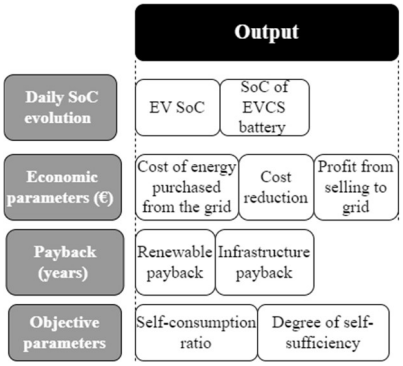

FIGURE 11. Output parameters of the simulator.

For each vehicle, the model assumes that several variables are in advance known, namely: (1) an initial SoC of the batteries, (2) daily rental's predicted periods (comprising the start and end of rental periods), and (3) a predicted set of routes between CSs during the day (comprising the estimated periods in transit between stations and periods parked at each CS). These variables can be estimated using information from previous rentals and must be updated throughout the day in a deployed situation.

B. OUTPUTS

The outputs of the simulator, represented in Fig.11, obtained in each simulation step of the system, are associated with the EVs, CSs, batteries, and effective charging periods. The data obtained during a rental day in the simulation can be divided in four main groups: (1) daily evolution SoC (translates the evolution of the SoC of the battery of each EV and CS in the system); (2) economic parameters (concerns the cost of purchasing energy from the grid, the amount of reduction costs obtained by not purchasing from the grid, and the profit from selling to the grid by injecting the surplus of energy); (3) payback metrics, and (4) energy flow parameters to evaluate the system operation. Points 3 and 4 were addressed in the previous section.

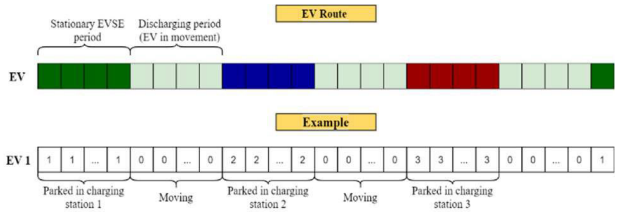

FIGURE 12. Data structures that store the expected location of each EV in the subsequent time periods.

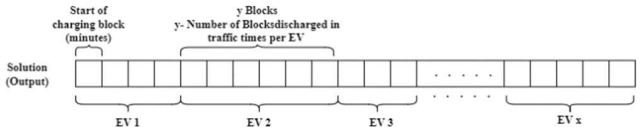

FIGURE 13. Data structure that stores the charging periods of each vehicle in DT CS system.

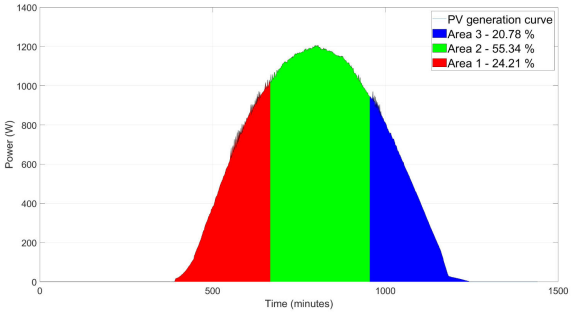

FIGURE 14. The probability of allocation of charging blocks result from the energy generated in each of the three periods shown.

C. SIMULATOR STAGES

After the definition of the input parameters of the system, in the following we define the funcioning of the system, which are key to obtain the results of that specific system.

The simulator assumes that the daily path of each vehicle is known a-priori. The daily routes of each vehicle can be obtained from a real distribution of paths of a daily rental or predicted using the information of earlier rentals.

Simulator's wise, the path for each EV is randomly generated at startup and stays the same during the whole simulation (it simulates one day of the system). The predicted or actual distance traveled by each car in one journey is used to define the number of charging blocks that each vehicle needs. The simulator uses blocks of 15 minutes for the temporal definition. Each EV has thus periods where it is transiting between stations and periods where it is at the CS. These distances between stations were obtained from a Gamma probability distribution. The value given by the Gamma distribution is divided by the average speed (of 22.5 km/h) to obtain the expected travel time (in hours) of each EV. By calculating the travel time, it is possible to divide the period of one day into the desired periods of time (15 minutes time blocks).

Fig.12 shows the structure of the data array that contains the expected daily path/states of the EV. In other words, the path is described by a set of states, whose values can vary between 0 and m, where m represents the total number of CSs. More precisely, state 0 means that the vehicle is moving between CSs, while states 1 to m, directly identify the CS number where the vehicle is. A vehicle cannot transit from two CSs without passing through state 0.

While the EV route structure defines the moments when the vehicle is traveling between CSs, or remains at a certain CS, it does not define when the vehicle is charging, because the allocation of charging blocks depends on an algorithm that performs charge scheduling. Fig.13 shows the structure of a solution for the DT CS system simulated. For each vehicle, the number of charging blocks is defined in accordance with the energy required to perform the predicted daily routine. The charging blocks must be allocated in some of the CSs where the EV passes, maximizing the use of renewable energy, considering the costs of purchasing and selling energy and considering all the limitations of the existing equipment at the stations, as explained in previous sections.

Charging periods can only be allocated when the vehicle is at a CS. The allocation of these charging blocks is generated pseudo randomly taking into consideration the PV power installed in each CS. So, at times of highest generation, the probability of allocation is greater. Each vehicle, from EV 1 to EV x, is associated with its specific number of charging blocks.

Out of the scope of this paper, as here the focus is the DT, the charging blocks allocation will take into consideration expected positioning of the vehicle (attained with machine learning) and optimization algorithms (using, e.g., genetic algorithms).

The charging block allocation was done considering a probability that reflects the distribution of the generated power. The curve: (1) was divided into three areas with equal periods (it was only considered periods when there is solar generation); (2) each area corresponds to a percentage of total generation; (3) considering those percentages, the charging blocks allocation is done. Those three main areas of probability distribution will help to understand and optimize the use of the generated energy. This division tends to be based on the position and intensity of the sun throughout the day, morning, midday and evening. Fig.14 represents that probability curve, in that specific PV curve the following percentages are: Area 1 - 24.21%; Area 2 - 55.34%; Area 3-20.78%. Percentages vary depending on the dinamics of PV generation.

After the allocation stage, simulation of one full day of the system operation will occur (from 0-24h). This simulation result in all the output parameters necessary to assess how beneficial the system is.

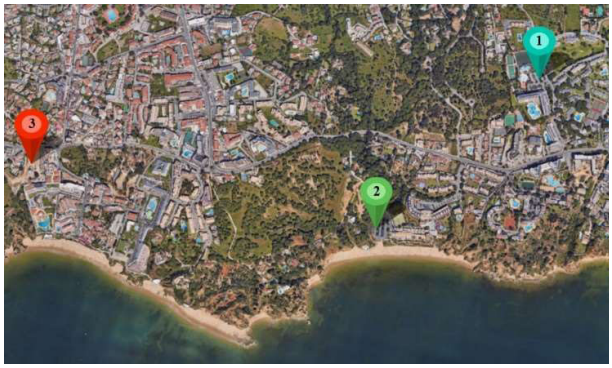

FIGURE 15. Location considered for the three CSs: 1 – In an area close to several Hotel units; 2 – St. Eulalia's beach; 3 – In an area with restaurants and bars. These locations translate the main points of interest in this urban touristic area in Albufeira.

FIGURE 16. Cyclomotor L2e-U from Passion Motorbike.

VI. TEST SCENARIO AND CONDITIONS

To evaluate the simulator of the charging system, characterized in the last sections, several test scenarios were considered. So, this section describes the conditions used in the simulation tests, using the simulator described in the last section, presents the test scenarios, together with a case study.

As a simulation setup, a DT of a system with 3 CSs and 10 EVs, was considered. These CSs were placed in touristic locations of Albufeira, Portugal, as shown in Fig.15 [62].

The L2e-U (SOBIC LIGHT) [63] cyclomotor was chosen as EV, reflecting the options taken in the TTUES project [64].

The L2e-U, shown in Fig.16, is developed by the project partner Passion Motorbike. The battery characteristics are summarized in Table 5, being the initial SoC of the EV 53%.

To quantify the savings and/or cost (in €) of the EV rental supplier, the tariff rates of the energy supplier need to be considered. To quantify the cost of the energy purchased, three-hour rates for January 2023 of the Portuguese supplier Energias de Portugal (EDP) [65] were taken into account, as presented in Table 6.

It is assumed that, as the generated power is made available to the user, savings are obtained by not purchasing the associated energy from the grid. Since the internal battery only charges with locally generated energy, it is considered that this energy translates a cost saving equal to the cost that would result from acquiring it from the supplier. The stored energy can be used in non-generation periods to charge the EVs. However, the associated economic value is only considered once, when charging the local battery.

Regarding the tariff periods, a daily cycle was considered, which in Portugal is divided into winter and summer periods, as shown in Fig.17.

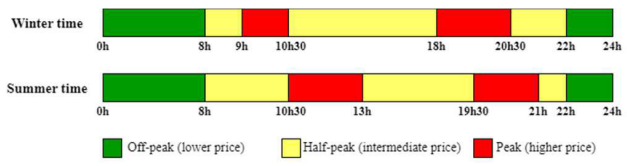

FIGURE 17. Periods of the considered tariff rate, based on a daily cycle (summer starts on the last Sunday of March; winter starts on the last Sunday of October).

To obtain the payback values and other desired financial parameters, cost values per kW of PV panels, and per kWh of local batteries, and from the EVs were obtained from a local equipment supplier. These values were: (1) 539 € (plus taxes) per kWp for the solar PV equipment and installation; and (2) 451 € (plus taxes) per kWh for the local storage and (3) 14500 € for the EV cost. For the computation of the infrastructure's payback, the following values were considered: (1) an equipment plus installation cost of 1500 €, which comprehends all hardware and materials needed for a CS (except the PV and battery); (2) a daily rental fee of an average amount of 30 € was considered; (3) annual maintenance cost of 500 € for each CS.

Regarding the PV generation, real generation data from a PV system that exists at the University of Algarve was used. The data used was obtained by randomly selecting 4 days in four months, namely: (1) 22nd of September 2022; (2) 21st of December 2022; (3) 26th of February 2023 and (4) 21st of June 2023. The variability in the PV generation dynamics can be observed in the generation levels shown in Fig.18. The installed system has a peak power of 54.2 kWp (172 panels of 315 Wp). Records of generation levels throughout the year show that the PV plant (including modules, inverters, and cabling) produces a peak power of approximately 40 kW, which corresponds to an efficiency of around 74% when compared with the installed peak power.

TABLE 5. Battery parameters (EV) input parameters (* [28]).

Parameters	Values
C_{bt}	94.580 Ah
C_{out}	45.000 Ah
$V_{bt,0}$	74.000V
K_{bt}	6.215×10^{-3} V*
A_{bt}	11.053 V*
B_{bt}	2.452 Ah^{-1}*
R_i	0.070 Ω*

TABLE 6. EDP tariffs prices (purchase and selling).

Time cycle		Purchase price (€)	Selling price (€)
		Three-hour rate tariffs (per/kWh)	
Out Off-peak	Peak	0.2864	0.170
	Half-Peak	0.1453	
Off-peak		0.0860	

The capacity of the PV unit that exists at the university was downscaled to 1:30 of its capacity, serving as base unitary size in the following computations.

In terms of the electrical losses of the battery charge controller, inverter and AC and DC cabling, an efficiency of 90% was considered for the DT.

Since the average daily paths of all EVs is a priori known, the required total number of charging blocks required in each station for a daily allocation can be computed. Given the required number of charging blocks in each CS, the size of the PV system to install in each CS can be obtained, by multiplying the base unitary size by a constant, so that the generated energy meets the required demand. In order to obtain these values, the simulator was executed 100 times. The results have shown that the total PV installation required for the system should be distributed among the stations according with the following ratios: CS 1- 67%; CS 2-19%; CS 3- 14%. Considering the predicted allocation of the charging blocks and the PV ratios, the constants that the PV reference curve must be multiplied by in each CS are represented in Table 7. That table also presents the storage capacity of the CS used in three different tests.

VII. RESULTS

In the following we describe the results obtained in the simulation of the system, translated by some of the variables of the EVs, CSs, and charging periods.

The data obtained from a simulated day comprehends: (1) the evolution of the SoC of the battery of each EV, including

TABLE 7. CS parameters.

	PV size (kWp)	Storage size (kWh)		
		Test 1	Test 2	Test 3
CS 1	3.533×base=4.946	3.00	6.00	0
CS 2	1.001×base=1.401	1.00	2.00	0
CS 3	0.738×base=1.033	1.00	2.00	0

in what CS they are in each period, (2) the evolution of the SoC of the battery of each CS, and (3) the evaluation parameters defined in Chapter IV.

To estimate the adequate level of storage in each of the CS, a comparison of the evaluation parameters will be made, taking into account the different local storage of the CSs presented in Table 6.

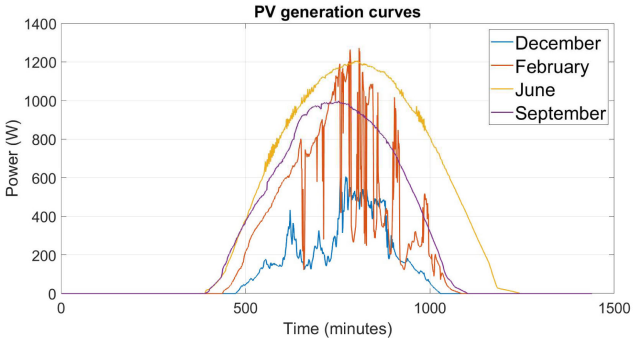

FIGURE 18. PV base curves from the correspondent months.

In Fig.19 the different energy flows in each CS are presented. The system has as primary requirement the fulfillment of the demand from the EVs, in terms of charging blocks allocation. The initial high allocation of charging blocks in CS 1 results from the fact that this is the starting point for every EV on the system, where there is a greater charging demand.

In Fig.20 the daily evolution of the SoC in each specific CS local battery is represented. The local batteries in the CS only charge with solar energy. This only occurs when the PV power exceeds the allocated power for the charging of EV and if the SoC of the CS local storage is not at its full capacity.

In the beginning of the day, all vehicles start at CS1, that is located close to the hotel units. There is no PV energy available, and the internal storage is at lowest point, so the demand required by the allocated charging blocks is fulfilled by the distribution grid. When the PV array begins generating power, since there is no energy at the CS's battery, the grid will fulfill the difference between the allocated and produced powers.

In periods where the PV generation is higher than the demand, the internal battery of the CS will charge (as can be verified in Fig.19, at around minute 550 for CS1).

Since in this simulation the allocations of charging blocks were done at the beginning of a day, there can be allocated blocks that are not effectively charged. This occurs when the SoC of EVs reaches 90%. One solution to avoid that situation and improve the system efficiency is the re-scheduling in different periods of the day, considering the updated values at that specific time.

Table 7 presents the evaluation parameters obtained for one simulated day of June with: CS1 - 3kWh; CS2 - 1kWh and CS3 - 1kWh. The values of the SC obtained in all CSs are relatively low. This results from the fact that there is a low correlation between generation and consumption. As can be verified, during many periods of the day, the generated power is not used, while in some other periods there are peaks in demand, much higher than the generation curve. A solution to improve these values would be to optimize the allocation of charging blocks, in order to take advantage of almost every moment of the day when there is generation. Increasing the number of EVs in the system could also help to contribute to a better use, as there is a greater use of generation and less moments without allocation of charging blocks.

The value of SS of the system is high, but there is still margin to increase it, by adding more storage capacity.

In order to know what the variation of the metrics would be used, one simulation was made for each month for all three storage sizes considered in Table 7. The results are shown in Tables 9, 10 and 11 translating the average values for the associated battery size, for all months. In Fig.21 the results of those tests are shown.

The increase of the capacity of the batteries has a direct effect on both energy flow metrics, however, can have a significant impact in the renewable payback (an increase of 33%) as a result from the high cost of battery units.

VIII. DISCUSSION

Analyzing the results obtained, it was noted that without batteries, the renewable payback is significantly reduced, however, the values of the SC and SS are negatively impacted, especially the SS.

It is therefore essential to align and improve all these system parameters in order to maximize the energy flow parameters and thus achieve an optimized system for improved results.

Some solutions can be applied and contribute to this end and may have to be considered for future developments: (1) Energy sharing solutions between CSs using the vehicles as energy conveyers and V2G, can increase the SC and reduce the need to be grid connected as well as the dependence on new investments in RES and local storage; (2) the optimization of the charging periods EV fleets require scheduling optimization algorithms that allow improving the allocation of the charging blocks along the day, for an optimized efficient operation of the system. This solution can also optimize the use of the RES in each CS, which can result in a reduction of the requirements regarding PV energy and local storage installation. As already mentioned, the optimization of the allocation is out of the scope of this paper and will be addressed in a future publication.

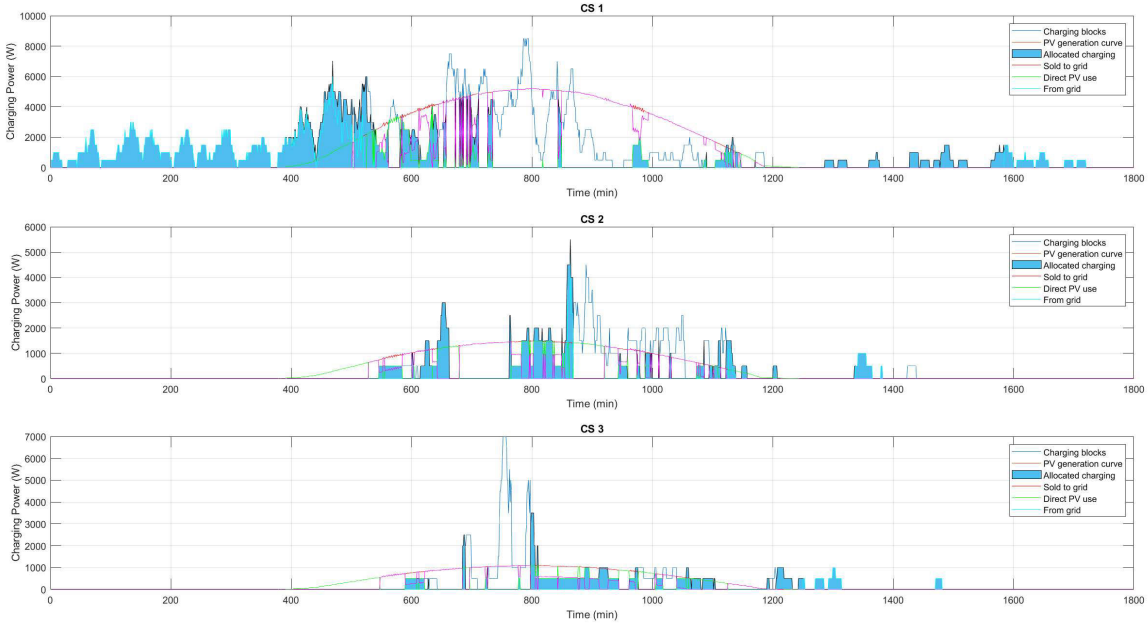

FIGURE 19. Scheduling result of the energy management system for the three CSs during one day of EV rentals of June in the CSs capacity test with: CS1-3kWh; CS2-1kWh and CS3-1kWh. The chart includes: (1) the charging blocks that resulted from the scheduling algorithm (dark blue trace); (2) the power expected from PV generation (red trace); (3) the effective charging blocks used by the EVs (blue fill); (4) the generated power that was directly consumed, represented as direct PV use (green trace) (5) the excess PV energy injected and sold to the distribution grid (purple trace); (6) the amount of energy that had to be demanded and consequently bought from the distribution grid, as a consequence of not having enough PV nor battery charge available (light blue trace).

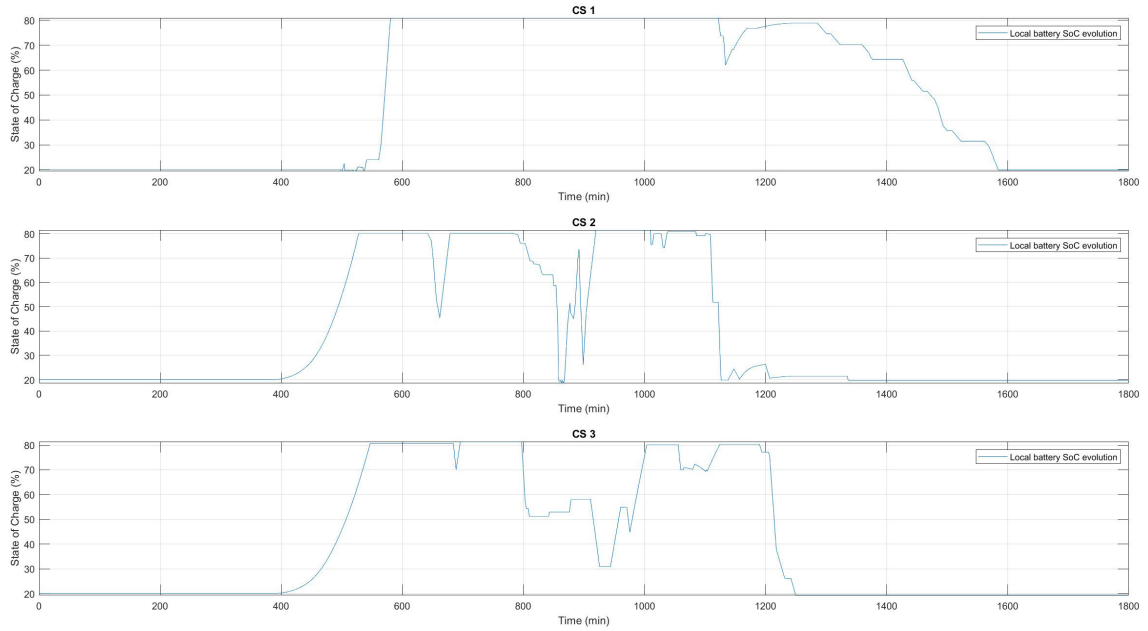

FIGURE 20. Daily evolution of the SOC of the internal batteries in the three CSs.

TABLE 8. Results of the test with battery sizes in cs of (3,1,1) KWH, month of june compreending economic, payback and objective parameters outputs of the simulation solution.

	Economic (in €)			Paybacks (in years)		Energy flow metrics (in %)	
	Purchased from grid	Saved with PV	Sold to grid	Renewable	Infra-structure	Self-consumption	Self-sufficiency
CS 1	1.330	1.141	5.470	2.302	4.475	47.029	83.112
CS 2	0.159	0.599	1.060	2.716		60.170	
CS 3	0.076	0.429	0.815	2.938		52.170	

TABLE 9. Results of the test with battery sizes in cs of (3,1,1) KWH compreending economic, payback and objective parameters outputs of the simulation solution (average of the four months chosen).

	Economic (in €)			Paybacks (in years)		Energy flow metrics (in %)	
	Purchased from grid	Saved with PV	Sold to grid	Renewable	Infra-structure	Self-consumption	Self-sufficiency
CS 1	1.648	0.873	3.069	5.413	4.658	46.470	76.951
CS 2	0.490	0.442	0.539	6.916		71.543	
CS 3	0.281	0.280	0.449	7.465		69.293	

TABLE 10. Results of the test with battery sizes in cs of (6,2,2) KWH compreending economic, payback and objective parameters outputs of the simulation solution (average of the four months chosen).

	Economic (in €)			Paybacks (in years)		Energy flow metrics (in %)	
	Purchased from grid	Saved with PV	Sold to grid	Renewable	Infra-structure	Self-consumption	Self-sufficiency
CS 1	1.528	0.982	3.056	6.553	4.727	46.854	78.760
CS 2	0.470	0.439	0.439	9.167		76.657	
CS 3	0.239	0.292	0.372	10.704		74.112	

TABLE 11. Results of the test with no batteries at cs compreending economic, payback and objective parameters outputs of the simulation solution (average of the four months chosen).

	Economic (in €)			Paybacks (in years)		Energy flow metrics (in %)	
	Purchased from grid	Saved with PV	Sold to grid	Renewable	Infra-structure	Self-consumption	Self-sufficiency
CS 1	2.424	1.037	3.800	2.974	4.523	29.707	67.853
CS 2	0.705	0.504	0.849	3.303		32.005	
CS 3	0.814	0.357	0.636	3.287		31.367	

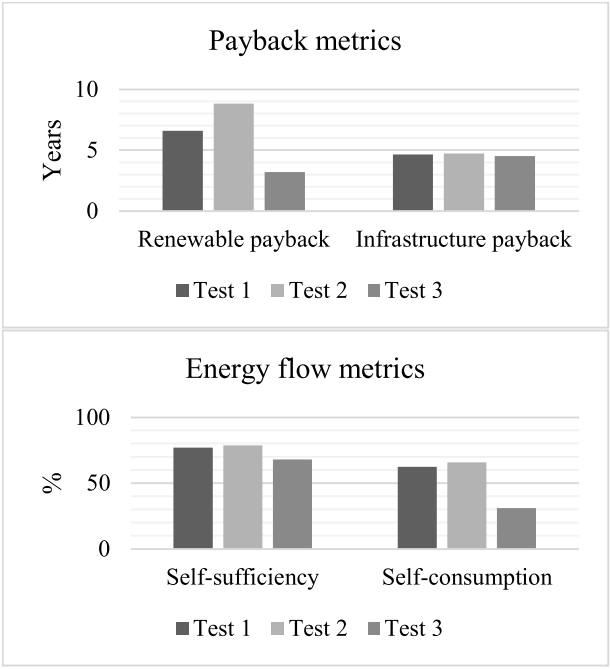

FIGURE 21. Results of the payback and energy flow metrics according with the three performed tests, defined in Table 7.

IX. CONCLUSION AND FUTURE DEVELOPMENT

The development of this simulator and the associated DT of CSs are an important step towards performing an optimized integration between EV charging processes and renewable generation.

The methodology allows selecting different input scenarios and/or several management strategies, assessing each one of them using a set of metrics. This allows selecting the solutions that could bring cost savings and that, at the same time, good operational efficiency, for companies managing EV fleets.

Using the DT, the performance of CSs can be made reflect real data from a real-world scenario, which can be updated regularly. This can also be used to decide what the best charge scheduling strategy.

Regarding the results of the performance evaluation metrics used, there is potential for further refinement in the DT system. Some strategies as integration of a multi-objective optimization algorithm process (considering the evaluation metrics used) for a more optimized charging block allocation, a better sizing of PV and local storage, together with the coexistence with V2G energy flow, could be the key to achieving a more optimized system.

In summary, this field holds immense potential for further advancements, and we remain committed to contributing to its ongoing progress.

REFERENCES

[1] R. G. Newell, D. Raimi, S. Villanueva, and B. C. Prest, "Global energy outlook 2020: Energy transition or energy addition?" *Resour. Futur.*, pp. 1–8, 2020.

[2] B. Xu, R. Zhong, G. Hochman, and K. Dong, "The environmental consequences of fossil fuels in China: National and regional perspectives," *Sustain. Develop.*, vol. 27, no. 5, pp. 826–837, Sep. 2019, doi: 10.1002/sd.1943.

[3] *Renewables 2022 Global Status Report*, Renewables Now (REN21), Paris, France, 2022.

[4] (2023). *PV Potential and Irradiation Can be Seen and Obtained From the Global Solar Atlas, Developed by Solargis, ESMAP and World Bank Group*. [Online]. Available: https://globalsolaratlas.info/map

[5] N. Mlilo, J. Brown, and T. Ahfock, "Impact of intermittent renewable energy generation penetration on the power system networks—A review," *Technol. Econ. Smart Grids Sustain. Energy*, vol. 6, no. 1, p. 123, Dec. 2021, doi: 10.1007/s40866-021-00123-w.

[6] R. P. Narasipuram and S. Mopidevi, "A technological overview & design considerations for developing electric vehicle charging stations," *J. Energy Storage*, vol. 43, Nov. 2021, Art. no. 103225, doi: 10.1016/j.est.2021.103225.

[7] A. Fathollahi, S. Y. Derakhshandeh, A. Ghiasian, and M. A. S. Masoum, "Optimal siting and sizing of wireless EV charging infrastructures considering traffic network and power distribution system," *IEEE Access*, vol. 10, pp. 117105–117117, 2022, doi: 10.1109/ACCESS.2022.3219055.

[8] M. Grieves and J. Vickers, "Digital twin: Mitigating unpredictable, undesirable emergent behavior in complex systems BT," in *Transdisciplinary Perspectives on Complex Systems: New Findings and Approaches*, F.-J. Kahlen, S. Flumerfelt, and A. Alves, Eds. Cham, Switzerland: Springer, 2017, pp. 85–113.

[9] F. Xiang, Z. Zhang, Y. Zuo, and F. Tao, "Digital twin driven green material optimal-selection towards sustainable manufacturing," *Proc. CIRP*, vol. 81, pp. 1290–1294, 2019, doi: 10.1016/j.procir.2019.04.015.

[10] M. Singh, E. Fuenmayor, E. Hinchy, Y. Qiao, N. Murray, and D. Devine, "Digital twin: Origin to future," *Appl. Syst. Innov.*, vol. 4, no. 2, p. 36, May 2021, doi: 10.3390/asi4020036.

[11] P. Huang, J. Munkhammar, R. Fachrizal, M. Lovati, X. Zhang, and Y. Sun, "Comparative studies of EV fleet smart charging approaches for demand response in solar-powered building communities," *Sustain. Cities Soc.*, vol. 85, Oct. 2022, Art. no. 104094, doi: 10.1016/j.scs.2022.104094.

[12] *Electric Vehicles From Life Cycle and Circular Economy Perspectives*, EEA, Liechtenstein, Europe, 2018.

[13] T. André, "Renewables 2021," Global Status Report, Renewables Now (REN21), Paris, France, Tech. Rep. REN21, 2021.

[14] P. Barman, L. Dutta, S. Bordoloi, A. Kalita, P. Buragohain, S. Bharali, and B. Azzopardi, "Renewable energy integration with electric vehicle technology: A review of the existing smart charging approaches," *Renew. Sustain. Energy Rev.*, vol. 183, Sep. 2023, Art. no. 113518, doi: 10.1016/j.rser.2023.113518.

[15] F. Mwasilu, J. J. Justo, E.-K. Kim, T. D. Do, and J.-W. Jung, "Electric vehicles and smart grid interaction: A review on vehicle to grid and renewable energy sources integration," *Renew. Sustain. Energy Rev.*, vol. 34, pp. 501–516, Jun. 2014, doi: 10.1016/j.rser.2014.03.031.

[16] H. Martin, R. Buffat, D. Bucher, J. Hamper, and M. Raubal, "Using rooftop photovoltaic generation to cover individual electric vehicle demand—A detailed case study," *Renew. Sustain. Energy Rev.*, vol. 157, Apr. 2022, Art. no. 111969, doi: 10.1016/j.rser.2021.111969.

[17] D. Thomas, V. Klonari, F. Vallée, and C. S. Ioakimidis, "Implementation of an e-bike sharing system: The effect on low voltage network using Pv and smart charging stations," in *Proc. Int. Conf. Renew. Energy Res. Appl. (ICRERA)*, Nov. 2015, pp. 572–577, doi: 10.1109/ICRERA.2015.7418478.

[18] S. S. Deshmukh and J. M. Pearce, "Electric vehicle charging potential from retail parking lot solar photovoltaic awnings," *Renew. Energy*, vol. 169, pp. 608–617, May 2021, doi: 10.1016/j.renene.2021.01.068.

[19] R. Dhawan and S. P. Karthikeyan, "An efficient EV fleet management for charging at workplace using solar energy," in *Proc. Nat. Power Eng. Conf. (NPEC)*, 2018, pp. 1–5, doi: 10.1109/NPEC.2018.8476746.

[20] A. R. Bhatti and Z. Salam, "A rule-based energy management scheme for uninterrupted electric vehicles charging at constant price using photovoltaic-grid system," *Renew. Energy*, vol. 125, pp. 384–400, Sep. 2018, doi: 10.1016/j.renene.2018.02.126.

[21] R. Fachrizal and J. Munkhammar, "Improved photovoltaic self-consumption in residential buildings with distributed and centralized smart charging of electric vehicles," *Energies*, vol. 13, no. 5, p. 1153, Mar. 2020, doi: 10.3390/en13051153.

[22] P. B. Suseela and C. V. K. Bhanu, "Design of solar-powered electric vehicle charging system," in *Proc. Int. Conf. Advancement Technol. (ICONAT)*, 2023, pp. 1–8, doi: 10.1109/ICONAT57137.2023.10080468.

[23] K. Hajar, B. Guo, A. Hably, and S. Bacha, "Smart charging impact on electric vehicles in presence of photovoltaics," in *Proc. 22nd IEEE Int. Conf. Ind. Technol. (ICIT)*, Valencia, Spain, Mar. 2021, pp. 643–648.

[24] A. Arancibia and K. Strunz, "Modeling of an electric vehicle charging station for fast DC charging," in *Proc. IEEE Int. Electr. Vehicle Conf.*, Mar. 2012, pp. 1–6, doi: 10.1109/IEVC.2012.6183232.

[25] D. Dallinger, S. Gerda, and M. Wietschel, "Integration of intermittent renewable power supply using grid-connected vehicles—A 2030 case study for California and Germany," *Appl. Energy*, vol. 104, pp. 666–682, Apr. 2013, doi: 10.1016/j.apenergy.2012.10.065.

[26] M. Bortolini, M. Gamberi, and A. Graziani, "Technical and economic design of photovoltaic and battery energy storage system," *Energy Convers. Manage.*, vol. 86, pp. 81–92, Oct. 2014, doi: 10.1016/j.enconman.2014.04.089.

[27] P. Bastida-Molina, E. Hurtado-Pérez, M. C. Moros Gómez, and C. Vargas-Salgado, "Multicriteria power generation planning and experimental verification of hybrid renewable energy systems for fast electric vehicle charging stations," *Renew. Energy*, vol. 179, pp. 737–755, Dec. 2021, doi: 10.1016/j.renene.2021.07.002.

[28] L. Valverde, F. Rosa, A. J. del Real, A. Arce, and C. Bordons, "Modeling, simulation and experimental set-up of a renewable hydrogen-based domestic microgrid," *Int. J. Hydrogen Energy*, vol. 38, no. 27, pp. 11672–11684, Sep. 2013, doi: 10.1016/j.ijhydene.2013.06.113.

[29] A. Fragaki and T. Markvart, "Stand-alone PV system design: Results using a new sizing approach," *Renew. Energy*, vol. 33, no. 1, pp. 162–167, Jan. 2008, doi: 10.1016/j.renene.2007.01.016.

[30] A. M. Ghazvini and J. Olamaei, "Optimal sizing of autonomous hybrid PV system with considerations for V2G parking lot as controllable load based on a heuristic optimization algorithm," *Sol. Energy*, vol. 184, pp. 30–39, May 2019, doi: 10.1016/j.solener.2019.03.087.

[31] S. Hussain, R. R. Irshad, F. Pallonetto, Q. Jan, S. Shukla, S. Thakur, J. G. Breslin, M. Marzband, Y.-S. Kim, M. A. Rathore, and H. El-Sayed, "Enhancing the efficiency of electric vehicles charging stations based on novel fuzzy integer linear programming," *IEEE Trans. Intell. Transp. Syst.*, vol. 24, no. 9, pp. 9150–9164, Sep. 2023, doi: 10.1109/TITS.2023.3274608.

[32] S. Hussain, M. A. Ahmed, and Y.-C. Kim, "Efficient power management algorithm based on fuzzy logic inference for electric vehicles parking lot," *IEEE Access*, vol. 7, pp. 65467–65485, 2019, doi: 10.1109/ACCESS.2019.2917297.

[33] S. Hussain, M. A. Ahmed, K.-B. Lee, and Y.-C. Kim, "Fuzzy logic weight based charging scheme for optimal distribution of charging power among electric vehicles in a parking lot," *Energies*, vol. 13, no. 12, p. 3119, Jun. 2020, doi: 10.3390/en13123119.

[34] S. Hussain, K.-B. Lee, M. A. Ahmed, B. Hayes, and Y.-C. Kim, "Two-stage fuzzy logic inference algorithm for maximizing the quality of performance under the operational constraints of power grid in electric vehicle parking lots," *Energies*, vol. 13, no. 18, p. 4634, Sep. 2020, doi: 10.3390/en13184634.

[35] Y. Dahmane, R. Chenouard, M. Ghanes, and M. Alvarado-Ruiz, "Optimized time step for electric vehicle charging optimization considering cost and temperature," *Sustain. Energy, Grids Netw.*, vol. 26, Jun. 2021, Art. no. 100468, doi: 10.1016/j.segan.2021.100468.

[36] F. G. Dias, M. Mohanpurkar, A. Medam, D. Scoffield, and R. Hovsapian, "Impact of controlled and uncontrolled charging of electrical vehicles on a residential distribution grid," in *Proc. IEEE Int. Conf. Probabilistic Methods Appl. Power Syst. (PMAPS)*, Jun. 2018, pp. 1–5, doi: 10.1109/PMAPS.2018.8440511.

[37] S. Deilami and S. M. Muyeen, "An insight into practical solutions for electric vehicle charging in smart grid," *Energies*, vol. 13, no. 7, p. 1545, Mar. 2020, doi: 10.3390/en13071545.

[38] *International Organization for Standardization's*, Standard ISO 15118, 2023. [Online]. Available: https://www.iso.org/home.html

[39] *International Electrotechnical Comission*, document IEC 61851, 2023. [Online]. Available: https://www.iec.ch/homepage

[40] J. Antoun, M. E. Kabir, B. Moussa, R. Atallah, and C. Assi, "A detailed security assessment of the EV charging ecosystem," *IEEE Netw.*, vol. 34, no. 3, pp. 200–207, May 2020, doi: 10.1109/MNET.001.1900348.

[41] M. Parchomiuk, A. Moradewicz, and H. Gawinski, "An overview of electric vehicles fast charging infrastructure," in *Proc. Prog. Appl. Elect. Eng. (PAEE)*, Jun. 2019, pp. 1–5, doi: 10.1109/PAEE.2019.8788983.

[42] O. Frendo, N. Gaertner, and H. Stuckenschmidt, "Real-time smart charging based on precomputed schedules," *IEEE Trans. Smart Grid*, vol. 10, no. 6, pp. 6921–6932, Nov. 2019, doi: 10.1109/TSG.2019.2914274.

[43] K. M. Tan, V. K. Ramachandaramurthy, and J. Y. Yong, "Integration of electric vehicles in smart grid: A review on vehicle to grid technologies and optimization techniques," *Renew. Sustain. Energy Rev.*, vol. 53, pp. 720–732, Jan. 2016, doi: 10.1016/j.rser.2015.09.012.
[44] N. El Sayed, "A prototypical implementation of an ISO-15118-based wireless vehicle to grid communication for authentication over decoupled technologies," in *Proc. AEIT Int. Conf. Elect. Electron. Technol. Automot. (AEIT AUTOMOTIVE)*, 2019, pp. 1–6.
[45] H. S. Das, M. M. Rahman, S. Li, and C. W. Tan, "Electric vehicles standards, charging infrastructure, and impact on grid integration: A technological review," *Renew. Sustain. Energy Rev.*, vol. 120, Mar. 2020, Art. no. 109618, doi: 10.1016/j.rser.2019.109618.
[46] R. Fachrizal, M. Shepero, D. van der Meer, J. Munkhammar, and J. Widén, "Smart charging of electric vehicles considering photovoltaic power production and electricity consumption: A review," *eTransportation*, vol. 4, May 2020, Art. no. 100056, doi: 10.1016/j.etran.2020.100056.
[47] J. Monteiro and M. S. Nunes, "A renewable source aware model for the charging of plug-in electrical vehicles," in *Proc. 1st Int. Conf. Vehicle Technol. Intell. Transp. Syst.*, 2015, pp. 51–58, doi: 10.5220/0005459000510058.
[48] B. D. Allen, "Digital twins and living models at NASA," NASA, Washington, DC, USA, Tech. Rep. 20210023699, 2021.
[49] K. Zhang, T. Qu, D. Zhou, H. Jiang, Y. Lin, P. Li, H. Guo, Y. Liu, C. Li, and G. Q. Huang, "Digital twin-based opti-state control method for a synchronized production operation system," *Robot. Comput.-Integr. Manuf.*, vol. 63, Jun. 2020, Art. no. 101892, doi: 10.1016/j.rcim.2019.101892.
[50] M. Grieves and J. Vickers, "Digital twin: Mitigating unpredictable, undesirable emergent behavior in complex systems," in *Transdisciplinary Perspectives on Complex Systems: New Findings and Approaches*. Cham, Switzerland: Springer, 2016.
[51] G. Yu, X. Ye, X. Xia, and Y. Chen, "Towards cognitive EV charging stations enabled by digital twin and parallel intelligence," in *Proc. IEEE 1st Int. Conf. Digit. Twins Parallel Intell. (DTPI)*, 2021, pp. 290–293, doi: 10.1109/DTPI52967.2021.9540103.
[52] Q. Lu, H. Jiang, S. Chen, Y. Gu, T. Gao, and J. Zhang, "Applications of digital twin system in a smart city system with multi-energy," in *Proc. IEEE 1st Int. Conf. Digit. Twins Parallel Intell. (DTPI)*, Jul. 2021, pp. 58–61, doi: 10.1109/DTPI52967.2021.9540135.
[53] W. A. Ali, M. Roccotelli, and M. P. Fanti, "Digital twin in intelligent transportation systems: A review," in *Proc. 8th Int. Conf. Control, Decis. Inf. Technol. (CoDIT)*, 2022, pp. 576–581, doi: 10.1109/CoDIT55151.2022.9804017.
[54] G. Bhatti, H. Mohan, and R. Raja Singh, "Towards the future of smart electric vehicles: Digital twin technology," *Renew. Sustain. Energy Rev.*, vol. 141, May 2021, Art. no. 110801, doi: 10.1016/j.rser.2021.110801.
[55] W. A. Ali, M. P. Fanti, M. Roccotelli, and L. Ranieri, "A review of digital twin technology for electric and autonomous vehicles," *Appl. Sci.*, vol. 13, no. 10, p. 5871, May 2023, doi: 10.3390/app13105871.
[56] C. Bordons, F. G. Torres, and M. A. Ridao, *Model Predictive Control of Micro-Grids*. Cham, Switzerland: Springer, 2019.
[57] O. Tremblay, L. A. Dessaint, and A. I. Dekkiche, "A generic battery model for the dynamic simulation of hybrid electric vehicles," in *Proc. IEEE Vehicle Power Propuls. Conf.*, Sep. 2007, pp. 284–289, doi: 10.1109/VPPC.2007.4544139.
[58] O. Tremblay and L.-A. Dessaint, "Experimental validation of a battery dynamic model for EV applications," *World Electr. Vehicle J.*, vol. 3, no. 2, pp. 289–298, Jun. 2009, doi: 10.3390/wevj3020289.
[59] C. M. Shepherd, "Design of primary and secondary cells," *J. Electrochem. Soc.*, vol. 112, no. 7, p. 657, 1965, doi: 10.1149/1.2423659.
[60] G. Merei, J. Moshövel, D. Magnor, and D. U. Sauer, "Optimization of self-consumption and techno-economic analysis of PV-battery systems in commercial applications," *Appl. Energy*, vol. 168, pp. 171–178, Apr. 2016, doi: 10.1016/j.apenergy.2016.01.083.
[61] R. Perez, L. Burtis, T. Hoff, S. Swanson, and C. Herig, "Quantifying residential PV economics in the U.S.—Payback vs cash flow determination of fair energy value," *Sol. Energy*, vol. 77, no. 4, pp. 363–366, Oct. 2004, doi: 10.1016/j.solener.2004.03.004.
[62] A. M. B. Francisco, "Coordinates, 37o05N 8o13W," Google Earth, Albufeira-Santa, Eulália Beach, Tech. Rep., Mar. 2023.
[63] A. M. B. Francisco. *Scoobic Light-Urban Mobility*. Accessed: Mar. 6, 2023. [Online]. Available: https://scoobic.com/light-es/
[64] A. M. B. Francisco. *TTUES-Transporte Turístico Urbano Eléctrico Sostenible*. Accessed: Feb. 1, 2021. [Online]. Available: https://www.t2ues.eu/
[65] A. M. B. Francisco. *Tarifarios*. Accessed: Mar. 6, 2023. [Online]. Available: https://www.edp.pt/particulares/energia/tarifarios/

ANDRÉ M. B. FRANCISCO received the B.Sc. degree in electrical and electronics engineering from the University of Algarve, in 2018, and the M.Sc. degree in electrical and electronics engineering and in information technologies and telecommunications, in 2020. He is currently pursuing the Ph.D. degree in electrical engineering with the University of Algarve. Currently, he has a Ph.D. individual research grant funded by the Portuguese Foundation for Science and Technology (FCT).

JÂNIO MONTEIRO received the Graduate degree in electrical and computers engineering from the University of Porto and the master's and Ph.D. degrees in electrical and computer engineering from Instituto Superior Técnico, University of Lisbon, Portugal. He is currently a Professor with the Institute of Engineering, Universidade do Algarve, Portugal. He is also the President of the Board of Directors of CINTAL, a Technological Research Center of the Algarve. His research interests include sensor networks, the Internet of Things, smart grids, communication networks, and machine learning. He is also a member of the Coordination Team of the Culatra 2030 Project, a Pilot Project supported by the Clean Energy for EU Islands Secretariat, and that aims to create a Sustainable Community in the Culatra Island, Portugal.

PEDRO J. S. CARDOSO received the B.Sc. degree in mathematics and in computer science from the University of Coimbra, Portugal, the M.Sc. degree in computational mathematics from the University of Minho, Portugal, and the Ph.D. degree in mathematics and in operations research from the University of Seville, Spain. He is currently an Associate Professor and a Researcher with the University of Algarve, where he works for more than two decades, a member of the Associate Laboratory of Robotics and Engineering Systems (LARSyS) and the Director of the Electrical Engineering Department, University of Algarve. He has broad knowledge in the fields of algorithms and data manipulation in general, with a particular emphasis in the field of machine learning and multiple objective meta-heuristics. Over the past years, he has been involved in over a dozen scientific and development projects, authored more than 90 publications, and an editor of over a dozen of books.